Asian Journal of Chemistry; Vol. 36, No. 5 (2024), 1135-1141

ASIAN JOURNAL OF CHEMISTRY

https://doi.org/10.14233/ajchem.2024.31388

Synthesis and *in silico* Assessment of Heteroaryl Semicarbazones: Towards Understanding Antimicrobial Activities and Safety Profiles

NIDAGURTHI GUGGULLA RAGHAVENDRA RAO[1], PRASHANTI CHITRAPU[2], GURINDERDEEP SINGH[3,*], SOWJANYA PULIPATI[4] and HARI VELURU[5]

[1]KIET School of Pharmacy, KIET group of Institutions, Delhi-NCR, Meerut Road (NH-58), Ghaziabad-201206, India
[2]Vision College of Pharmaceutical Sciences and Research, Secunderabad-500092, India
[3]Department of Pharmaceutical Sciences and Drug Research, Punjabi University, Patiala-147002, India
[4]Department of Pharmaceutics, Vignan Pharmacy College, Vadlamudi-522213, Guntur (Dist), India
[5]MB School of Pharmaceutical Sciences, Mohan Babu University, Tirupati-517503, India

*Corresponding author: E-mail: gdspharma4@gmail.com

Received: 13 February 2024; *Accepted*: 29 March 2024; *Published online*: 30 April 2024; AJC-21620

Seven semicarbazone derivatives incorporating either substituted furan or thiophene were synthesized by reacting phenylurea with semicarbazide and various heteroaryl aldehydes. The newly synthesized compounds were characterized using IR, NMR, mass spectrometry and elemental analysis. Additionally, their antibacterial and anti-tubercular activities were also evaluated. *In silico* tools such as Swiss ADME and Pro Tox II were employed to assess molecular targets, medicinal chemistry properties, as well as toxicity and safety profiles. Compounds **3a-g** demonstrated significant antibacterial activity at a 100 µg/mL when compared to the standard ciprofloxacin. Notably, compounds **3c**, **3d**, **3f** and **3g** exhibited the highest activity against all bacterial strains. Furthermore, compound **3d** demonstrated anti-tubercular activity at all tested concentrations.

Keywords: Heteroaryl semicarbazones, *In silico* safety profiling, Antibacterial activity, Antitubercular activity.

INTRODUCTION

In response to the persistent challenges posed by infectious diseases, especially in the wake of the recent COVID-19 pandemic, the need to address bacterial and microbial infections, including tuberculosis, has become increasingly urgent. The emergence of multi-drug resistant strains further complicates treatment regimens, necessitating innovative approaches in antimicrobial drug discovery [1,2]. Despite considerable progress, tuberculosis remains a formidable global health concern, imposing a substantial burden on public health systems. The prevalence of the disease persists and the rise of drug-resistant strains poses a significant obstacle in the effective treatment. Moreover, the concurrent occurrence of bacterial and microbial infections, as witnessed during the COVID-19 pandemic, accentuates the need for versatile and potent therapeutic agents [3,4].

In pursuit of developing novel antimicrobial agents with enhanced efficacy and safety profiles, the exploration of heteroaryl semicarbazones has emerged as a promising avenue within medicinal chemistry [5]. Semicarbazones, characterized by a hydrazine-derived moiety, exhibit diverse pharmacological properties and their structural modification with heteroaryl substituents holds promise for imparting unique bioactive features [6-9]. Studies on semicarbazones have unveiled their potential as antimicrobial [10,11], antiviral [12], anticancer [13], anticonvulsant [14], analgesic and anti-inflammatory [15] agents. Their mechanism of action often involves interactions with essential biological macromolecules, such as proteins and nucleic acids. Additionally, semicarbazones have demonstrated chelating properties, making them relevant in the metal coordination chemistry [16].

The strategic structural modification of semicarbazones through the introduction of heteroaryl substituents offers a unique approach to fine-tune their pharmacological properties. Heteroaryl groups, such as furan and thiophene, are well-known in medicinal chemistry for their distinctive electronic

and steric effects. The integration of these heterocyclic moieties into semicarbazones imparts additional structural diversity, potentially influencing the compounds' solubility, lipophilicity and overall bioavailability [17].

In present studies, we employ *in silico* methods to assess the toxicity and safety profiles of the synthesized heteroaryl semicarbazones. Traditionally, the evaluation of toxicity and safety relied heavily on the time-consuming and resource intensive *in vivo* and *in vitro* experiments. *In silico* methods, however, leverage computational models to simulate and predict the interactions between chemical entities and biological systems, providing a rapid and cost-effective means of assessing potential risks associated with novel compounds [18]. Furthermore, *in silico* approaches allow for the early identification of potential safety concerns during the drug development process, enabling the modification or elimination of compounds with undesirable properties before progressing to costly and time consuming preclinical and clinical phases.

Considering this information and with the aim of developing effective antimicrobial substances, the current study is focussed on the synthesis of a novel series of heteroaryl semicarbazones (**3a-g**) incorporating furan and thiophene as structural components. In addition to synthesis, the *in vitro* antibacterial activity of the compounds was also evaluated against four bacterial strains, whereas the antitubercular activity was assessed using the microplate alamar blue assay. Furthermore, the study employed *in silico* methods to predict the toxicity and safety profile of the synthesized compounds.

EXPERIMENTAL

The chemicals employed in this study were procured from commercial suppliers and used in the synthesis of the compounds without further purification. Melting points of the synthesized compounds were measured using the open capillary method and remain uncorrected. The progress of reactions was moni-tored *via* thin layer chromatography (TLC) using precoated silica gel strips. A solvent system with a 2:1 ratio of hexane to ethyl acetate was applied and chromatographic spots were visualized using an ultraviolet chamber.

Characterization: FT-IR spectra were obtained using a SHIMADZU FT-IR 4000 instrument equipped with KBr disks. Mass spectra were acquired with a JEOL GC mate II GC-Mass spectrometer operating at 70 eV, utilizing the direct insertion probe method for detailed information on molecular weights and fragmentation patterns. For ^{1}H NMR spectra, a BRUKER AVIII-500 MHz FT-NMR spectrometer was employed and a JEOL ECZ 400S spectrometer was used for collecting ^{13}C NMR spectra. Tetramethylsilane served as the internal standard and dimethylsulfoxide was the chosen solvent.

Synthesis of phenyl semicarbazide: Phenyl urea (**1**, 0.1 mol) dissolved in 30 mL of ethanol in 50 mL round bottomed flask was added to an equimolar amount of hydrazine hydrate solution. To promote the reaction, 4 g of NaOH was introduced and this alkaline reaction mixture was subsequently refluxed for 2 h under a condenser for continuous reaction. Following refluxing, the mixture was cooled in an ice bath. The resulting product was filtered under suction to separate the solid product from the reaction mixture. The isolated product was further purified through recrystallization from ethanol to obtain white crystals. Yield: 72%; m.p.: 168-171 ºC. IR (KBr, ν_{max}, cm^{-1}): 1662 (C=O), 1536 (C=C) and 1590 (C-N), MS (*m/z*, %): 151.07 (M+); ^{1}H NMR (DMSO-d_6, δ ppm): 7.08 (1H, tt), 7.20-7.43 (4H, 7.27 (dd), 7.36 (dd).

Synthesis of heteroaryl semicarbazones (3a-g): A condensation reaction was initiated by dissolving phenyl semicarbazide (**2**) in 50 mL of ethanol and then heteroaryl aldehyde was introduced into the reaction mixture along with 1 mL of glacial acetic acid as catalyst. The reaction undergoes reflux at 45 ºC for 1 h, ensuring the efficient progression of the reaction transformation. Following reflux, the mixture was subjected to magnetic stirring at room temperature for an additional 15 min. The solid product, which separates out during the reaction, was collected and further purified through crystallization from ethanol (**Scheme-I**). Confirmation of the purity of all the synthesized compounds was achieved through thin-layer chromatography (TLC) utilizing a mobile phase consisting of hexane and ethyl acetate mixture.

1-[-Furan-2-ylmethylideneamino]-3-phenylurea (3a): Yield: 64%: m.p.: 189-192 ºC; FT-IR (KBr, ν_{max}, cm^{-1}): 3207 (N-H), 1612 (C=C), 1648 (C=O); ^{1}H NMR (DMSO-d_6, δ ppm): 6.30 (1H, dd), 6.88 (1H, dd), 7.08 (1H, tt), 7.20-7.48 (5H, dd), 7.27 (dd), 7.37 (dd), 7.42 (dd), 7.84 (1H, s); ^{13}C NMR (DMSO-

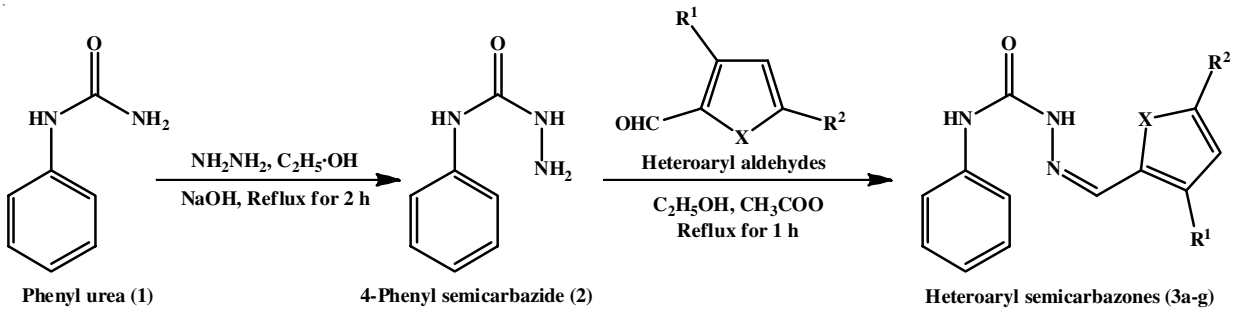

3a: X = O, $R^1 = R^2 = -H$
3b: X = O, $R^1 = -H$, $R^2 = -NO_2$
3c: X = O, $R^1 = -H$, $R^2 = -CH_3$
3d: X = O, $R^1 = -H$, $R^2 = -CH_2OH$
3e: X = S, $R^1 = R^2 = -H$
3f: X = S, $R^1 = -H$, $R^2 = -CH_3$
3g: X = S, $R^1 = -CH_3$, $R^2 = -H$

Scheme-I: Synthesis of heteroaryl semicarbazones (**3a-g**)

d_6, δ ppm): 112.0 (1C, s), 113.7 (1C, s), 119.9 (2C, s), 127.8 (1C, s), 128.2 (2C, s), 134.2 (1C, s), 134.8 (1C, s), 143.6 (1C, s), 148.7 (1C, s), 149.6 (1C, s); MS (*m/z*, %): 229.05 (M+); Anal. calcd. (found) % for $C_{12}H_{11}N_3O_2$: C, 62.87 (62.91); H, 4.84 (4.87); N, 18.33 (18.35); O, 13.96 (13.92).

1-[(5-Nitrofuran-2-yl)methylideneamino]-3-phenylurea (3b): Yield: 68 %: m.p.: 213-215 ºC; FT-IR (KBr, ν_{max}, cm^{-1}): 3384 (N-H), 1674 (C=N), 1726 (C=C), 1652 (C=O), 1496 (NO_2); ^{1}H NMR (DMSO-d_6, δ ppm): 7.02-7.43 (7H, 7.08, tt), 7.08 (d), 7.17 (d), 7.27 (dd), 7.37 (dd), 8.24 (1H, s); ^{13}C NMR (DMSO-d_6, δ ppm): 113.6 (1C, s), 118.2 (1C, s), 119.9 (2C, s), 127.8 (1C, s), 128.2 (2C, s), 134.2 (1C, s), 134.8 (1C, s), 149.6 (1C, s), 150.1 (1C, s), 156.1 (1C, s); MS (*m/z*, %): 274.06 (M+); Anal. calcd. (found) % for $C_{12}H_{10}N_4O_4$: C, 52.56 (52.54); H, 3.68 (3.66); N, 20.43 (20.45); O, 23.34 (23.36).

1-[(5-Methylfuran-2-yl)methylideneamino]-3-phenylurea (3c): Yield: 72%: m.p.: 173-175 ºC; FT-IR (KBr, ν_{max}, cm^{-1}): 3268 (N-H), 1635 (C=N), 1562 (C=C), 1607 (C=O), 2874 (C-H); ^{1}H NMR (DMSO-d_6, δ ppm): 2.29 (3H, s), 6.13 (1H, d), 6.79 (1H, d), 7.08 (1H, tt), 7.20-7.43 (4H, 7.27, dd), 7.37 (dd), 7.86 (1H, s); ^{13}C NMR (DMSO-d_6, δ ppm): 13.5 (1C, s), 107.9 (1C, s), 112.6 (1C, s), 119.9 (2C, s), 127.8 (1C, s), 128.2 (2C, s), 134.2 (1C, s), 134.8 (1C, s), 149.6 (1C, s), 150.1 (1C, s), 151.7 (1C, s); MS (*m/z*, %): 243.12 (M+); Anal. calcd. (found) % for $C_{13}H_{13}N_3O_2$: C, 64.19 (64.21); H, 5.39 (5.36); N, 17.27 (17.29); O, 13.15 (13.18).

1-[(5-Hydroxy methylfuran-2-yl)methylideneamino]-3-phenylurea (3d): Yield: 65%: m.p.: 182-185 ºC; FT-IR (KBr, ν_{max}, cm^{-1}): 3380 (N-H), 1664 (C=N), 1528 (C=C), 1604 (C=O), 2908 (C-H), 3518 (OH); ^{1}H NMR (DMSO-d_6, δ ppm): 4.49 (2H, s), 6.24 (1H, d), 6.82 (1H, d), 7.08 (1H, tt), 7.20-7.43 (4H), 7.27 (dd), 7.37 (dd), 7.88 (1H, s); ^{13}C NMR (DMSO-d_6, δ ppm): 56.0 (1C, s), 110.3 (1C, s), 112.8 (1C, s), 119.6 (2C, s), 127.4 (1C, s), 128.4 (2C, s), 134.3 (1C, s), 134.9 (1C, s), 149.6 (1C, s), 150.1 (1C, s), 155.6 (1C, s); MS (*m/z*, %): 259.08 (M+); Anal. calcd. (found) % for $C_{13}H_{13}N_3O_3$: C, 60.22 (60.24); H, 5.05 (5.07); N, 16.21 (16.23); O, 18.51 (18.49).

1-Phenyl-3-(thiophen-2-ylmethylideneamino)phenylurea (3e): Yield: 62%: m.p.: 197-200 ºC; FT-IR (KBr, ν_{max}, cm^{-1}): 3325 (N-H), 1636 (C=N), 1566 (C=C), 1647 (C=O), 722 (C-S); ^{1}H NMR (DMSO-d_6, δ ppm): 6.95-7.14 (3H, 7.01 (dd), 7.03 (dd), 7.08 (tt), 7.20-7.43 (5H), 7.27 (dd), 7.31 (dd), 7.37 (dd), 8.10 (1H, s); ^{13}C NMR (DMSO-d_6, δ ppm): 119.9 (2C, s), 127.5 (1C, s), 127.7-127.8 (2C, 127.7 (s), 127.8 (s), 128.2 (2C, s), 131.9 (1C, s), 134.2 (1C, s), 143.2 (1C, s), 144.0 (1C, s), 149.6 (1C, s); MS (*m/z*, %): 245.06 (M+); Anal. calcd. (found) % for $C_{12}H_{11}N_3OS$: C, 58.76 (58.79); H, 4.52 (4.54); N, 17.13 (17.15); O, 6.52 (6.55); S, 13.07 (13.08).

1-[(5-Methylthiophen-2-yl)methylideneamino]-3-phenylurea (3f): Yield: 70%: m.p.: 207-210 ºC; FT-IR (KBr, ν_{max}, cm^{-1}): 3348 (N-H), 1674 (C=N), 1573 (C=C), 1605 (C=O), 736 (C-S); ^{1}H NMR (DMSO-d_6, δ ppm): 2.27 (3H, s), 6.93 (1H, d), 7.08 (1H, tt), 7.20-7.43 (5H), 7.27 (dd), 7.31 (d), 7.37 (dd), 8.09 (1H, s); ^{13}C NMR (DMSO-d_6, δ ppm): 15.4 (1C, s), 119.9 (2C, s), 125.7 (1C, s), 127.8 (1C, s), 128.2 (2C, s), 132.6 (1C, s), 134.2 (1C, s), 139.5 (1C, s), 143.2 (1C, s), 144.0 (1C, s), 149.6 (1C, s); MS (*m/z*, %): 259.08 (M+); Anal. calcd. (found) % for $C_{13}H_{13}N_3OS$: C, 60.21 (60.25); H, 5.05 (5.08); N, 16.20 (16.24); O, 6.17 (6.19); S, 12.36 (12.33).

1-[(3-Methylthiophen-2-yl)methylideneamino]-3-phenylurea (3g): Yield: 68%: m.p.: 185-187 ºC; FT-IR (KBr, ν_{max}, cm^{-1}): 3352 (N-H), 1676 (C=N), 1573 (C=C), 1608 (C=O), 732 (C-S); ^{1}H NMR (DMSO-d_6, δ ppm): 2.22 (3H, s), 6.97-7.14 (2H, 7.03 (d), 7.08 (tt), 7.18-7.43 (5H), 7.24 (d), 7.27 (dd), 7.37 (dd), 8.06 (1H, s); ^{13}C NMR (DMSO-d_6, δ ppm): 15.8 (1C, s), 119.9 (2C, s), 125.4 (1C, s), 127.8 (1C, s), 128.2 (2C, s), 130.4 (1C, s), 134.2 (1C, s), 136.5 (1C, s), 143.2 (1C, s), 143.8 (1C, s), 149.6 (1C, s); MS (*m/z*, %): 259.09 (M+); Anal. calcd. (found) % for $C_{13}H_{13}N_3OS$: C, 60.21 (60.18); H, 5.05 (5.03); N, 16.20 (16.22); O, 6.17 (6.19); S, 12.36 (12.38).

In silico toxicity assessment

Protox II: To assess the potential toxicities of the selected molecules, Protox II, a toxicity prediction tool, was utilized in this study [19]. Computational models within Protox II were employed to predict oral toxicological endpoints, including carcinogenicity, mutagenicity and hepatotoxicity. The selected molecules were input into the Protox II tool and predictions were obtained for each toxicity endpoint. The tool leverages established algorithms and databases, providing insights into potential adverse effects associated with the investigated molecules.

Swiss ADME: The Swiss ADME online platform's prediction tools were employed for a comprehensive evaluation of various molecular characteristics [20]. This encompassed physicochemical properties, lipophilicity, water solubility, pharmacokinetics, druglikeness, molecular target and medicinal chemistry parameters. Specifically, *in silico* absorption, distribution, metabolism, excretion and toxicity (ADMET) predictions were conducted for the synthesized compounds **4a-g** using the Swiss ADME software. This computational approach facilitates a detailed understanding of the compounds' druglikeness, contributing to the assessment of their potential as pharmacologically viable entities.

Antimicrobial activity

Antitubercular activity: The antitubercular activity of the synthesized heteroaryl semicarbazones (**4a-g**) was evaluated using the microplate Alamar blue assay method (MABA). The *M. tuberculosis* H37 RV strain served as the test pathogen, with isonicotinic acid hydrazide (INH) as the reference drug. A sterile 96-well plate was prepared, with the outermost wells filled with sterile deionized water to prevent medium evaporation. Middlebrook 7H9 (MB 7H9) broth (100 µL) was distributed into each well and the synthesized compounds were serially diluted on the plate. The antitubercular activity was assessed at drug concentrations ranging from 0.2 to 100 µg/mL. Plates were incubated and Alamar blue reagent was added after 5 days. Interpretation was based on colour changes, where blue indicated no bacterial growth and pink signified bacterial growth [21].

Antibacterial activity: Compounds **4a-g** were evaluated for antibacterial activity using the agar cup plate method against a spectrum of Gram-negative (*Escherichia coli*, *Pseudomonas aeruginosa*) and Gram-positive (*Staphylococcus epidermatitis*,

Bacillus subtilis) organisms. The minimum inhibitory concentration (MIC) method was employed, with ciprofloxacin as a reference standard. Brain heart infusion agar was used and colonies were visually aligned with a 0.5 McFarland turbidity standard. The agar plate was uniformly streaked and wells were created using a hollow tube. Different volumes of synthesized compounds were added to the wells and the plates were incubated. The inhibition zone diameter was measured after 24 h and MIC was determined through serial dilutions. This approach allowed for a comprehensive assessment of antibacterial efficacy [22].

RESULTS AND DISCUSSION

The synthetic pathway employed for the preparation of the heteroaryl semicarbazones (**3a-g**) is depicted in **Scheme-I**. The synthesis involved the condensation reaction of phenylurea (**1**) and hydrazine followed by the subsequent reaction of phenyl semicarbazide (**2**) with heteroarylaldehydes. To ensure the purity of the synthesized compounds, thin-layer chromatography (TLC) was utilized using hexane and ethyl acetate solvent mixture as mobile phase. Furthermore, each synthesized compound exhibited distinctive peaks in both FT-IR and NMR spectra, providing robust evidence of their structural integrity. Mass spectra analysis further confirmed the presence of the anticipated molecular ion peak (M+) fragments, corroborating the successful synthesis of the titled heteroaryl semicarbazones.

Toxicity studies: In the assessment of potential oral toxicity risks associated with the synthesized heteroaryl semicarbazones (**3a-g**), Protox II, a toxicity prediction tool, was employed to evaluate various toxicological parameters such as carcinogenicity, mutagenicity and hepatotoxicity as outlined in Table-1. The *in silico* predictions using Protox II provide a detailed overview of the potential toxicological effects for each compound. Specifically, compound **3a** is predicted to exhibit active hepatotoxicity, carcinogenicity and cytotoxicity, whereas compound **3b** is projected as non-hepatotoxic but displays active carcinogenicity and mutagenicity. Compounds **3c** and **3d** exhibit both hepatotoxicity and carcinogenicity, whereas compounds **3e-g**, which contain a thiophenyl group, display moderate hepatotoxicity but are non-carcinogenic. Moreover, these compounds also show no immunotoxicity, mutagenicity or cytotoxicity. The LD_{50} values offer insights into acute toxicity levels. These predictions serve as an initial guide, underscoring the necessity for further experimental validation and exploration of structure-

TABLE-1
ORAL TOXICITY REPORT OF HETEROARYL SEMICARBAZONES (**3a-g**)

Compound	Target	Prediction	Probability	LD_{50} (mg/kg)	Toxicity class
3a	Hepatotoxicity	Active	0.67	752	4
	Carcinogenicity	Active	0.75		
	Immunotoxicity	Inactive	0.99		
	Mutagenicity	Inactive	0.55		
	Cytotoxicity	Inactive	0.82		
3b	Hepatotoxicity	Inactive	0.56	500	4
	Carcinogenicity	Active	0.91		
	Immunotoxicity	Inactive	0.96		
	Mutagenicity	Active	0.96		
	Cytotoxicity	Inactive	0.78		
3c	Hepatotoxicity	Active	0.64	752	4
	Carcinogenicity	Active	0.72		
	Immunotoxicity	Inactive	0.96		
	Mutagenicity	Inactive	0.68		
	Cytotoxicity	Inactive	0.74		
3d	Hepatotoxicity	Active	0.52	1000	4
	Carcinogenicity	Active	0.68		
	Immunotoxicity	Inactive	0.99		
	Mutagenicity	Inactive	0.52		
	Cytotoxicity	Inactive	0.78		
3e	Hepatotoxicity	Active	0.68	226	3
	Carcinogenicity	Active	0.72		
	Immunotoxicity	Inactive	0.99		
	Mutagenicity	Inactive	0.56		
	Cytotoxicity	Inactive	0.78		
3f	Hepatotoxicity	Active	0.67	226	3
	Carcinogenicity	Active	0.72		
	Immunotoxicity	Inactive	0.99		
	Mutagenicity	Inactive	0.55		
	Cytotoxicity	Inactive	0.79		
3g	Hepatotoxicity	Active	0.63	226	3
	Carcinogenicity	Active	0.70		
	Immunotoxicity	Inactive	0.93		
	Mutagenicity	Inactive	0.53		
	Cytotoxicity	Inactive	0.80		

activity relationships to enhance the understanding of safety profiles.

The physico-chemical properties predicted by Swiss ADME for the synthesized heteroaryl semicarbazones (**3a-g**) are shown in Table-2. The predicted physico-chemical properties, including flexibility, hydrogen bond characteristics, lipophilicity and sp^3 hybridized carbons, hold significant implications for the pharmacological behaviour of the synthesized heteroaryl semicarbazones (**3a-g**). The degree of flexibility, as indicated by the number of rotatable bonds, influences the compounds' ability to adopt different conformations, potentially impacting their interaction with biological targets. The compounds exhibit varying degrees of flexibility with compound **3a** showing moderate flexibility, while compound **3b** displays higher flexibility with six rotatable bonds. Hydrogen bond acceptors and donors play a crucial role in forming interactions with biological molecules, suggesting potential binding sites and modes of action. The numbers of hydrogen bond acceptors and donors differ among the compounds, with compounds **3b** and **3d** having higher counts, suggesting potential interactions with biological targets. Lipophilicity affects a compound's solubility and bioavailability, influencing its distribution within the body and varies from moderate to high, with compounds **3b** and **3d** being less lipophilic, which can impact their solubility and bioavailability.

Fraction Csp^3 is a metric used to quantify the degree of saturation or unsaturation in a molecular structure. It represents the proportion of sp^3 hybridized carbon atoms (saturated carbons) relative to the total number of carbon atoms in a molecule. This metric is relevant in medicinal chemistry and drug design, where it is used to assess the "alkylness" or degree of saturation in a compound. The fraction Csp^3 values indicate the proportion of sp^3-hybridized carbon atoms, with compounds **3c** and **3d** having a slightly higher fraction. Compounds with higher fraction Csp^3 values are often considered more drug-like, as they resemble natural products and existing drugs.

The pharmacokinetic and medicinal chemistry properties predicted by Swiss ADME for the synthesized heteroaryl semicarbazones (**3a-g**) are presented in Table-3, offering valuable insights into their potential drug-like characteristics. The GIA (gastro-intestinal absorption) values for all compounds are predicted to be high, suggesting favourable absorption in the gastrointestinal tract. This is a positive indicator for oral drug administration, as high GIA values correlate with enhanced bioavailability.

These predictions indicate that compounds **3a**, **3c** and **3d** are expected to penetrate the Blood-Brain Barrier (BBB). The BBB penetration suggests that these compounds may have the potential to cross the blood-brain barrier, which is significant, especially in the context of targeting central nervous system infections. The ability to traverse the BBB allows for potential therapeutic effects within the brain and central nervous system. P-gp (P-glycoprotein) substrate prediction indicates that none of the compounds are likely substrates for P-glycoprotein. This is relevant in drug development, as P-glycoprotein can influence drug absorption and distribution. Similarly, all compounds exhibit negative LogKp values, suggesting limited skin permeability. This is beneficial for drugs intended for systemic circulation rather than topical application.

Druglikeness predictions are affirmative for all the synthesized compounds, implying their adherence to drug-like properties. This is crucial in pharmaceutical development, as drug-like compounds are more likely to progress through further stages of drug discovery. The synthetic accessibility (SA) values, indicative of the ease of chemical synthesis, are within a reasonable range for all compounds. This suggests that the synthesis of these heteroaryl semicarbazones is feasible. The molecular target affinity predictions for the synthesized heteroaryl semi-

TABLE-2
PHYSICO-CHEMICAL PROPERTIES PREDICTED BY SWISS ADME

Compound	Rotatable bonds (flexibility)	Hydrogen bond acceptors	Hydrogen bond donors	Log Po/w	Fraction Csp^3
3a	5	3	2	1.89	0.00
3b	6	5	2	1.42	0.00
3c	5	3	2	2.25	0.08
3d	6	4	3	1.45	0.08
3e	5	2	2	2.56	0.00
3f	5	2	2	2.80	0.08
3g	5	2	2	2.78	0.08

TABLE-3
PREDICTION OF PHARMACOKINETIC AND MEDICINAL CHEMISTRY PROPERTIES USING SWISS ADME

Compound	GIA[a]	BBBP[b]	P-gpS[c]	LogKp(cm/s)[d]	BAS[e]	Druglikeness	SA[f]
3a	High	Yes	No	-5.91	0.55	Yes	2.89
3b	High	No	No	-6.42	0.55	Yes	3.06
3c	High	Yes	No	-5.71	0.55	Yes	3.03
3d	High	No	No	-6.70	0.55	Yes	3.13
3e	High	No	No	-5.57	0.55	Yes	2.71
3f	High	No	No	-5.77	0.55	Yes	2.86
3g	High	No	No	-5.79	0.55	Yes	2.84

a = Gastrointestinal absorption, b = Blood brain barrier permeant, c = P-gp substrate, d = Skin permeant, e = Bioavailability score and f = Synthetic accessibility

carbazones (**3a-g**) are shown in Fig. 1. The values represent the percentage of affinity towards various biological targets, including kinases, GPCRs (G protein-coupled receptors), oxidoreductases, nuclear receptors and lyases.

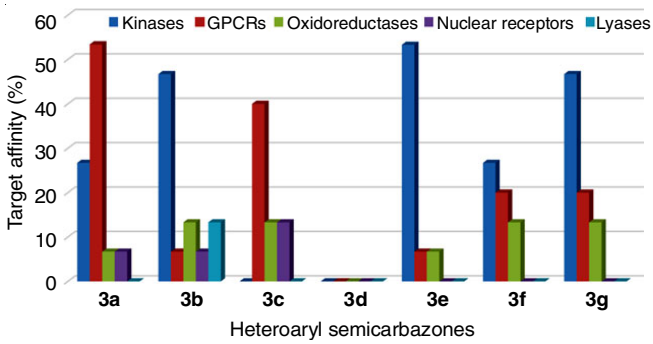

Fig. 1. Molecular target affinity of heteroaryl semicarbazones

Compound **3a** shows notable affinity for kinases and GPCRs, suggesting a potential role in modulating cellular signaling and surface receptor interactions. Compounds **3e**, **3f** and **3g** exhibit significant affinity towards kinases, pointing to their potential involvement in various cellular processes. Compound **3b** displays a broad spectrum of affinity, including kinases, GPCRs, oxidoreductases, nuclear receptors and lyases, indicating a diverse range of potential biological activities. The substantial lyase affinity suggests its potential role in metabolic processes. Compound **3c**, on the other hand, shows affinity for GPCRs, oxidoreductases and nuclear receptors, revealing potential interactions with these specific biological targets.

It is significant that compound **3d** did not produce any anticipated targets as per the Swiss Target Prediction program. This result emphasizes the uniqueness of compound **3d** and while the absence of predicted targets doesn't diminish its potential therapeutic value, further experimental validation is crucial to unravel its pharmacological activities and identify potential targets. This emphasizes the need for continued investigation to comprehensively understand the compound's mode of action and therapeutic potential.

Antimicrobial activity: All the synthesized heteroaryl semicrbazones (**3a-g**) underwent screening to evaluate their antitubercular and antibacterial activities. The antitubercular activity of the synthesized heteroaryl semicarbazones (**3a-g**) was evaluated against *Mycobacterium tuberculosis* H37Rv in Middlebrook 7H9 broth media (MB 7H9 broth), with isoniazid as standard drug (Table-4). Among the synthesized compounds, compound **3d**, characterized by a hydroxymethyl group on the furan moiety, demonstrated activity at concentrations of 25, 50 and 100 µg/mL. The presence of a hydroxymethyl group, with its electron-donating nature and hydrogen-bonding capabilities, may contribute to the distinct activity observed for this compound. However, the remaining compounds exhibited no significant activity at concentrations below 50 µg/mL. Notably, all the synthesized compounds were inactive at concentrations under 25 µg/mL compared to the standard drug isoniazid. Compound **3b**, containing a strongly electron withdrawing and ring deactivator nitro group on the furan ring, showed inactivity

TABLE-4
ANTI-TUBERCULAR ACTIVITY OF
HETEROARYL SEMICARBAZONES (**3a-g**)

Compound	Minimum inhibitory concentration		
	25 µg/mL	50 µg/mL	100 µg/mL
3a	R	S	S
3b	R	R	R
3c	R	S	S
3d	S	S	S
3e	R	R	S
3f	R	S	S
3g	R	S	S
INH	S	S	S

at all tested concentrations. This emphasizes the pivotal role of the aromatic ring system in the synthesized compounds for antitubercular activity, suggesting that groups enhancing aromaticity hold promise for the development of these compounds as potential antitubercular agents.

Significant variations in the antitubercular activity were observed among the bioisosteres **3a** and **3e**, which bear unsubstituted furan and thiophenyl moieties, respectively, at a concentration of 50 µg/mL. Interestingly, contrary to this observation, positional isomers (**3f** and **3g**) and bioisosteres (**3c** and **3f**) revealed noteworthy antitubercular activity at the same concentration of 50 µg/mL. The difference in activity between these compounds underscores the significance of the structural nuances in determining their effectiveness against *M. tuberculosis*. This emphasizes the necessity for additional investigation to understand the links between their structure and activity, which govern their antitubercular capabilities.

The antibacterial activity of all the synthesized compounds (**3a-g**) was evaluated using the agar cup-plate method, with ciprofloxacin as reference standard. Significant antibacterial activity was observed at a dose level of 100 µg, as depicted in Fig. 2. Compounds **3c**, **3d**, **3f** and **3g** exhibited the highest activity against the tested bacterial strains, potentially due to the presence of distinct electronically active groups, particularly the methyl and hydroxymethyl groups on the furan and thiophene rings. Furthermore, all the compounds exhibited significant antibacterial activity against different bacterial strains, which can be related to the variety of heteroaryl substituents present at the semicarbazone nitrogen. The phenyl semicarbazide moiety also contributed to their antibacterial properties.

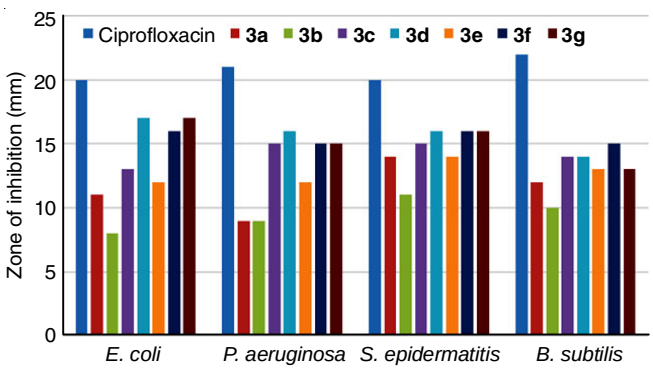

Fig. 2. Antibacterial activity of synthesized compounds **3a-g**

Conclusion

In conclusion, the synthesis and characterization of seven heteroaryl semicarbazone derivatives (**3a-g**) incorporating substituted furan or thiophene moieties have been successfully carried out. The antibacterial activity demonstrated the significant activity, particularly compounds **3c**, **3d**, **3f** and **3g** exhibiting significant efficacy against various bacterial strains. Moreover, compound **3d** displayed promising anti-tubercular activity at all tested concentrations, suggesting a diversified therapeutic potential. The utilization of *in silico* tools, including Swiss ADME and Pro Tox II, facilitated the exploration of molecular targets, medicinal chemistry properties and toxicity profiles suggest that these newly synthesized heteroaryl semicarbazones hold promise for lead optimization studies, presenting avenues for the development of improved and safer drugs. Further investigations, including additional pharmacological assays and optimization efforts, are warranted to fully realize the potential of these compounds in the realm of drug discovery and development.

ACKNOWLEDGEMENTS

The authors are thankful to their respective institutes for providing the research laboratory and computational facilities. Thanks are also due to Pro Tox II and Swiss ADME for providing free softwares and Government Dental College and Research Institute, Bellary, India for the antimicrobial analysis.

CONFLICT OF INTEREST

The authors declare that there is no conflict of interests regarding the publication of this article.

REFERENCES

1. K.A. Alene, K. Wangdi and A.C.A. Clements, *Trop. Med. Infect. Dis.*, **5**, 123 (2020); https://doi.org/10.3390/tropicalmed5030123
2. R. Crisan-Dabija, C. Grigorescu, C.A. Pavel, B. Artene, I.V. Popa, A. Cernomaz and A. Burlacu, *Can. Respir. J.*, 1401053 (2020); https://doi.org/10.1155/2020/1401053.
3. M.N. Hoque, S. Akter, I.D. Mishu, M.R. Islam, M.S. Rahman, M. Akhter, I. Islam, M.M. Hasan, M.M. Rahaman, M. Sultana, T. Islam and M.A. Hossain, *Microb. Pathog*., **156**, 104941 (2021); https://doi.org/10.1016/j.micpath.2021.104941
4. M.N. Hoque, S. Akter, I.D. Mishu, M.R. Islam, M.S. Rahman, M. Akhter, I. Islam, M.M. Hasan, M.M. Rahaman, M. Sultana, T. Islam and M.A. Hossain, *Microb. Pathog*., **156**, 104941 (2021); https://doi.org/10.1016/j.micpath.2021.104941
5. Z. Breijyeh and R. Karaman, *Antibiotics*, **12**, 628 (2023); https://doi.org/10.3390/antibiotics12030628
6. L. Jafri, F.L. Ansari, M. Jamil, S. Kalsoom, S. Qureishi and B. Mirza, *Chem. Biol. Drug Des.*, **79**, 950 (2012); https://doi.org/10.1111/j.1747-0285.2012.01360.x
7. H. Rajak, D.K. Jain, S. Singh, A. Singh, V.K. Patel, R. Veerasamy and R.S. Pawar, *Cent. Nerv. Syst. Agents Med. Chem.*, **17**, 64 (2017); https://doi.org/10.2174/1871524916666160330122625
8. A. Kumar, K. Lal, M. Yadav, S. Kumar, M.B. Singh and K. Kumari, *J. Mol. Struct.*, **1287**, 135660 (2023); https://doi.org/10.1016/j.molstruc.2023.135660
9. M. Marinescu, *Antibiotics*, **10**, 1002 (2021); https://doi.org/10.3390/antibiotics 10081002
10. M.B. Zivkovic, I.T. Novakovic, I.Z. Matic, D.M. Sladic and N.M. Krstic, *Steroids*, **148**, 36 (2019); https://doi.org/10.1016/j.steroids.2019.04.010
11. M. Sayed, A.M.K. El-Dean, M. Ahmed and R. Hassanien, *Synth. Commun.*, **48**, 413 (2018); https://doi.org/10.1080/00397911.2017.1403627
12. V. Francesconi, E. Cichero, S. Schenone, L. Naesens and M. Tonelli, *Molecules*, **25**, 1487 (2020); https://doi.org/10.3390/molecules25071487
13. J. Ma, X. Ni, Y. Gao, K. Huang, Y. Wang, J. Liu and G. Gong, *Chem. Pharm. Bull. (Tokyo)*, **67**, 351 (2019); https://doi.org/10.1248/cpb.c18-00738
14. M.J. Ahsan, *Cent. Nerv. Syst. Agents Med. Chem.*, **13**, 148 (2013); https://doi.org/10.2174/18715249113136660016
15. A. Rineh, N. Mahmoodi, M. Abdollahi, A. Foroumadi, M. Sorkhi and A. Shafiee, *Arch. Pharm.*, **340**, 409 (2007); https://doi.org/10.1002/ardp.200700045
16. I.A. Mir, Q. Ul Ain, T. Qadir, A.Q. Malik, S. Jan, S. Shahverdi and S.A. Nabi, *J. Mole. Struct.*, **1295**, 136216 (2024); https://doi.org/10.1016/ j.mol struc. 2023. 13 6216
17. J. Jampilek, *Molecules*, **24**, 3839 (2019); https://doi.org/10.3390/molecules2421383 9
18. D. Krewski, D. Acosta Jr., M. Andersen, H. Anderson, J.C. Bailar 3rd, K. Boekelheide, R. Brent, G. Charnley, V.G. Cheung, S. Green Jr., K.T. Kelsey, N.I. Kerkvliet, A.A. Li, L. McCray, O. Meyer, R.D. Patterson, W. Pennie, R.A. Scala, G.M. Solomon, M. Stephens, J. Yager and L. Zeise, *J. Toxicol. Environ. Health B Crit. Rev.*, **13**, 51 (2010); https://doi.org/10.1080/10937404.2010.483176
19. P. Banerjee, A.O. Eckert, A.K. Schrey and R. Preissner, *Nucleic Acids Res.*, **46(W1)**, W257 (2018); https://doi.org/10.1093/nar/gky318
20. A. Daina, O. Michielin and V. Zoete, *Sci. Rep.*, **7**, 42717 (2017); https://doi.org/10.1038/ srep42717
21. S.G. Franzblau, R.S. Witzig, J.C. McLaughlin, *J. Clin. Microbiol.*, **36**, 362 (1998); https://doi.org/10.112 8/JCM.36.2.362-366.1998
22. CLSI, M100 Performance Standards for Antimicrobial Susceptibility Testing, CLSI; Wayne, PA, USA, edn. 29 (2019).